

## Molecular dynamics and analytical Langevin equation approach for the self-diffusion constant of an anisotropic fluid

Pedro J. Colmenares, Floralba López, and Wilmer Olivares-Rivas\*  
*Quimicofísica de Fluidos y Fenómenos Interfaciales (QUIFFIS), Departamento de Química,*  
*Universidad de Los Andes, Mérida 5101, Venezuela*  
 (Received 17 July 2009; published 16 December 2009)

We carried out a molecular-dynamics (MD) study of the self-diffusion tensor of a Lennard-Jones-type fluid, confined in a slit pore with attractive walls. We developed Bayesian equations, which modify the virtual layer sampling method proposed by Liu, Harder, and Berne (LHB) [P. Liu, E. Harder, and B. J. Berne, *J. Phys. Chem. B* **108**, 6595 (2004)]. Additionally, we obtained an analytical solution for the corresponding nonhomogeneous Langevin equation. The expressions found for the mean-squared displacement in the layers contain naturally a modification due to the mean force in the transverse component in terms of the anisotropic diffusion constants and mean exit time. Instead of running a time consuming dual MD-Langevin simulation dynamics, as proposed by LHB, our expression was used to fit the MD data in the entire survival time interval not only for the parallel but also for the perpendicular direction. The only fitting parameter was the diffusion constant in each layer.

DOI: [10.1103/PhysRevE.80.061123](https://doi.org/10.1103/PhysRevE.80.061123)

PACS number(s): 02.50.-r, 02.70.-c, 05.10.Gg, 47.10.-g

### I. INTRODUCTION

With the advent of nanoscience and its technological implications, there has been a particular interest in getting a deeper insight on the dynamics of fluids confined in nanostructures. The behavior of the transverse diffusion constant of the fluid, under the geometrical constraint imposed by the confinement, has been studied in a number of ways. Statistical-mechanics theories, such as mode coupling analysis [2,3], memory function approach [4], lattice Boltzmann method [5], replica Ornstein-Zernike equation [6], and molecular modeling [1,7–11], have been used. Also effective transverse diffusion constants have been calculated from the mean first passage times, using a combination of Smoluchowski equation and the hypernetted-chain theory [12,13]. The technical difficulties of getting reliable experimental data enhance the interest on theoretical calculations. This work deals with the molecular-dynamics (MD) calculation of the anisotropic diffusion constant of a Lennard-Jones (LJ) fluid, confined between two attractive infinite planar sheets, separated at a given distance. Unlike the free diffusion case, here, the diffusion constant is position dependent, due to the potential exerted by the walls on the fluid. Fluid particles cannot span all phase space as the free diffusion particles do and, therefore, Kubo relation is no longer valid. In spite of this, one can still resort to MD modeling as a tool to predict diffusion transport properties, if the anisotropy of the system is carefully considered. In the analysis of the liquid-vapor water interface, Liu, Harder, and Berne (LHB) [1] introduced a dual simulation algorithm to overcome this difficulty. They matched dynamical properties, calculated with MD, with those determined by a trial-and-error Langevin-like dynamics, in which the diffusion constant was the *ad hoc* parameter of the calculation. Here, we propose an alternative direct method, combining the MD simulation with analytical solu-

tion of the stochastic differential equations of the problem, to bypass the numerical Langevin dynamics (LD) proposed by Liu *et al.* As we will show later in this paper, the method is simple, fast, and reliable in predicting position-dependent diffusion constants.

This paper is organized as follows. In Sec. II, we describe the evaluation of dynamical quantities, such as the mean-squared displacement (MSD), within virtual layers of the anisotropic fluid. In Sec. III, we decouple the Langevin equation to propose a set of stochastic differential equations, which incorporates in a natural way the anisotropy of the medium. We derive analytical formulas for the parallel and perpendicular MSD to be used as fitting functions of the numerical MD MSD data. We show that our more general equations reduce to LHB equations when the diffusion tensor is diagonal and show the correct time limiting behavior in the presence of the external force induced by the pore walls. Finally, in Sec. IV, we report the results for the position-dependent diffusion constants, for a specific case study of a dense interacting fluid.

### II. MOLECULAR-DYNAMICS EVALUATION OF MSD IN VIRTUAL LAYERS

In this section, we revisit the work of Liu *et al.* (LHB) [1] for the evaluation of the MSD for molecules in a virtual slit. As a case study, we used a system very similar to that studied before by Thomas and McGaughey [10]. It is a fluid confined in a pore, which consists of two infinite smeared molecular layers separated by a distance  $H$ . The fluid is composed of Lennard-Jones argonlike atoms of diameter  $\sigma$  and mass  $m$ , free to move in the  $x$  and  $y$  directions, parallel to the planes, but restricted to diffuse in the domain  $[0, H]$ , along the  $z$  direction. We follow a procedure similar to that of LHB in the sense that we assume the friction coefficient does not vary appreciably, for a given layer of width  $L$ , located between the positions  $z=z_a$  and  $z=z_b=z_a+L$ , parallel to the surface.

\*Corresponding author; wilmer@ula.ve

Formally, the MSD in the generic direction  $q$ , either  $x$ ,  $y$ , or  $z$ , is given by

$$\langle [q(t) - q_0]^2 \rangle = \int d\vec{r} \int d\vec{r}_0 [q(t) - q_0]^2 P(\vec{r}, t, \vec{r}_0), \quad (1)$$

where  $P(\vec{r}, t, \vec{r}_0)$  is the joint probability of finding a particle at position  $\vec{r}_0$  at time  $t=0$  and then at position  $\vec{r}$  at time  $t$ . Since the movement in the  $z$  direction is assumed to be independent of the movement in the  $x$  and  $y$  directions, the joint probability  $P(\vec{r}, t, \vec{r}_0)$  can be approximated as a coupled superposition,

$$P(\vec{r}, t, \vec{r}_0) = P(x, t, x_0; z_0) P(y, t, y_0; z_0) P(z, t, z_0), \quad (2)$$

where the presence of the variable  $z_0$  in  $P(q, t, q_0; z_0)$ , for  $q = \{x, y\}$  remarks the fact that the probability of displacement on  $q$  directions depends on the initial position in  $z$  since it is a functional of the local density, which in turn is a function of  $z$ . Keeping this in mind, we can further rewrite Eq. (2) in terms of Bayesian conditional probabilities

$$P(\vec{r}, t, \vec{r}_0) = P(x, t | x_0; z_0) P(y, t | y_0; z_0) P(z, t | z_0) g(z_0), \quad (3)$$

where, for example,  $P(x, t | x_0; z_0)$  is the conditional probability that the particle is located at  $x$  at time  $t$ , given that it was at  $x_0$  at time  $t=0$ , in a layer containing  $z_0$ .  $g(z_0)$  is the probability for a particle to be at position  $z_0$  at time  $t=0$ . It can be obtained directly from the local particle density  $\rho(z)$ . Substituting Eq. (3) into Eq. (1) and taking into account the independence of the integration variables, we find that the MSD along  $x$ ,  $y$ , and  $z$  for particles within a virtual layer of width  $L$ , are given by

$$\begin{aligned} \langle (\Delta x)^2 \rangle_L &= \int_{z_a}^{z_b} dz \int_{z_a}^{z_b} dz_0 P(z, t | z_0) g(z_0) \\ &\quad \times \left\{ \int_{-\infty}^{\infty} dx \int_{-\infty}^{\infty} dx_0 (\Delta x)^2 P(x, t | x_0; z_0) \right\} N_y(t; z_0), \\ \langle (\Delta y)^2 \rangle_L &= \int_{z_a}^{z_b} dz \int_{z_a}^{z_b} dz_0 P(z, t | z_0) g(z_0) \\ &\quad \times \left\{ \int_{-\infty}^{\infty} dy \int_{-\infty}^{\infty} dy_0 (\Delta y)^2 P(y, t | y_0; z_0) \right\} N_x(t; z_0), \\ \langle (\Delta z)^2 \rangle_L &= \int_{z_a}^{z_b} dz \int_{z_a}^{z_b} dz_0 P(z, t | z_0) g(z_0) (\Delta z)^2 N_x(t; z_0) N_y(t; z_0), \end{aligned} \quad (4)$$

where  $\Delta q = q(t) - q_0$ , and the factors  $N_q(t; z_0)$  for  $x$  and  $y$  are

$$N_q(t; z_0) = \int_{-\infty}^{\infty} dq \int_{-\infty}^{\infty} dq_0 P(q, t | q_0; z_0). \quad (5)$$

Since these factors correspond to the normalization of the probability in the  $x$  and  $y$  directions, they are set equal to one to get

$$\langle (\Delta x)^2 \rangle_L = \int_{z_a}^{z_b} dz \int_{z_a}^{z_b} dz_0 P(z, t | z_0) g(z_0) \{ \overline{(\Delta x)^2} \}, \quad (6)$$

$$\langle (\Delta y)^2 \rangle_L = \int_{z_a}^{z_b} dz \int_{z_a}^{z_b} dz_0 P(z, t | z_0) g(z_0) \{ \overline{(\Delta y)^2} \}, \quad (7)$$

$$\langle (\Delta z)^2 \rangle_L = \int_{z_a}^{z_b} dz \int_{z_a}^{z_b} dz_0 P(z, t | z_0) g(z_0) (\Delta z)^2, \quad (8)$$

where

$$\overline{(\Delta q)^2} = \int_{-\infty}^{\infty} dq \int_{-\infty}^{\infty} dq_0 (q(t) - q_0)^2 P(q, t | q_0; z_0), \quad (9)$$

for  $q = \{x, y\}$ . The result in Eqs. (6)–(8) is physically sound. It states that the MSD in the  $z$  direction is obtained averaging  $[z(t) - z_0]^2$  for molecules that remain during the time interval  $t$  in the layer, irrespective of its position in the  $x$  and  $y$  directions. While the MSD in the  $x$  and  $y$  directions are obtained averaging  $[x(t) - x_0]^2$  and  $[y(t) - y_0]^2$  over all values of  $x$  and  $y$ , subjected to the condition that the particles remain in the layer  $[z_a, z_b]$  in the  $z$  direction. We do not write Eqs. (6) and (7) as  $2P(t)D_{qq}t$  for  $x$  and  $y$ , as in Eq. (13) of Ref. [1], because there is a small dependence of the terms in braces on the position  $z_0$  and, above all, because—as we shall discuss in the next section—those terms converge to the bulk value  $2D^0t$  only for a free diffusing Brownian particle in an infinitely large layer, at an infinite time. Particles escape from finite layers if the time becomes too large.

To numerically evaluate these quantities in the MD simulation, we chose a simple model, similar to that used by Thomas and McGaughey [10], i.e., a LJ 12–6 system, describing argon atoms at a given temperature and density, confined by attractive LJ parallel walls [14–17]. We have carried out MD simulations for a fluid with bulk-reduced density  $\rho^* = 0.69$ , at a reduced temperature  $T^* = k_B T / \epsilon_{FF} = 0.75$ . For computational simplicity and without loss of generality, we have used a LJ 9–3 wall-fluid potential, corresponding to a smoothed wall interacting with a LJ fluid particle [14–17]. This potential has been used in the description of phase behavior and dynamics of fluids and colloidal suspensions in nanopores [18, 19]. It also mimics the hydrophobic interaction of a hydrocarbon wall with the oxygen atom of a water molecule [16, 17].

The method presented in this work is independent of the system under study, but the virtual layer treatment is conditioned by the magnitude of  $\epsilon_{WF}$  since it determines the local-density profiles and, therefore, the magnitude of the mean force  $F(z)$  acting on the diffusing particles. For sampling virtual layers close to a very attractive wall, the fluid becomes highly nonhomogeneous. This is illustrated in Fig. 1, where we plot the reduced local density and mean force, as a function of the position  $z$ , for a wall with  $\epsilon_{WF} = 1.0k_B T$ . The set of sampling virtual layers, of width  $0.5\sigma$ , beginning at  $z = 0.5\sigma$ , is also shown. Here the continuous line is  $\rho^*(z) = \rho(z)\sigma^3$ , the reduced local density of particles; the dashed line is the reduced mean force  $F^*(z) = \sigma\beta F(z)$ , due to the attractive walls, acting on a fluid particle located at  $z$ . It is obtained as the gradient of the potential of mean force, determined from the local density, as  $\beta F(z) = -d\beta W(z)/dz = d \ln \rho(z)/dz$ . For the temperature and density of the fluid and the characteristics of the interactions chosen [10], the

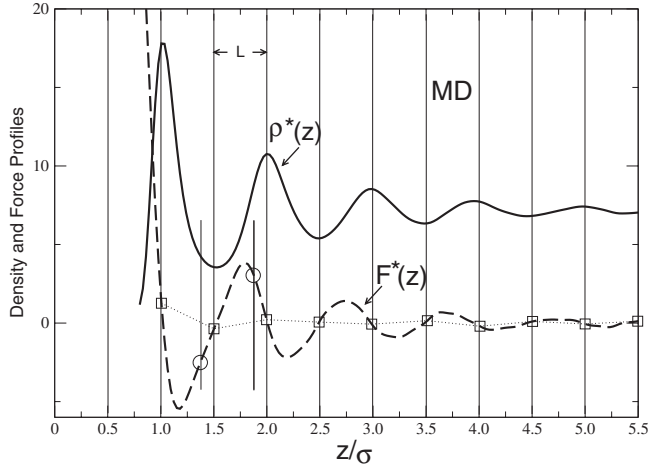


FIG. 1. Molecular-dynamics nonhomogeneous functions in the neighborhood of the walls, as a function of the reduced distance  $z/\sigma$ . For  $H=40\sigma$ ,  $\rho^*=0.69$ ,  $T^*=0.75$ , and  $\epsilon_{WF}=1.0k_B T$ . The solid line is the reduced local particle density  $\rho^*(z)=\rho(z)\sigma^3$  scaled by a factor of 10; the dashed line is the reduced mean force  $F^*(z)=\sigma\beta F(z)$ . The vertical lines denote the boundaries of a set of virtual layers of width  $L=0.5\sigma$  beginning at  $z_a=0.5\sigma$ . The squares  $\square$  denote the reduced force at the boundaries.

mean force is a strongly oscillating function of the position with respect to the walls.

Although not shown, we ran MD simulations for different values of the LJ 9–3  $\epsilon_{WF}$ . The so-called *more-wetting* value used by Thomas and McGaughey [10],  $\epsilon_{WF}=3.16k_B T$ , gives sharp local-density peaks next to the surface, close to a solidlike behavior, with very large values of  $F(z)$ . While the *less-wetting* value  $\epsilon_{WF}=0.45k_B T$  gives a low varying density profile showing—instead—a tendency to drying [20]. Since we are interested in the study of the effect of confinement on the anisotropic diffusion [12,13], we need to ensure a good phase behavior even for confined fluids in the nanopore regime [20]. Hence, to test the technique, we have chosen an intermediate  $\epsilon_{WF}=1.0k_B T$  value, between the less and more-wetting conditions, which corresponds to a typical liquid profile next to a solid surface, as shown in Fig. 1.

We proceed as follows. After thermal equilibration, the simulation time is denoted by  $s$ . The total simulation time is partitioned in  $J$  blocks of length  $n_{\max}\Delta s$ , where  $n_{\max}$  is the maximum number of time steps  $\Delta s$  in each block. Let us then consider the set of particles that stay in a layer of width  $L$ , i.e.,  $z(t) \in [z_a, z_a + L]$ , during the time interval  $t$ , between the simulation time  $s_0$  and  $s=s_0+t$ . The initial number of particles in the layer at  $s=s_0$  is  $N(0)=N(s_0)$ , and the number of particles in the set, still in the layer after the interval  $t$ , is  $N(t)=N(s_0+t)$ . If the MD simulation time step is  $\Delta s$ , the time interval after  $n$  steps is  $t=n\Delta s$ . The maximum time interval used to evaluate quantities inside the layers was  $t_{\max}=n_{\max}\Delta s$ . After  $n_{\max}$  steps, the algorithm is reinitiated to measure the dynamics in the layer, setting  $s_0=s$  again. This layer sampling is repeated  $J$  times. We denote the number of particles in the set that stay in a layer in the  $j$ th layer sampling or repetition as  $N_j(s)$ .

The MSD in the  $j$ th layer sampling is evaluated summing over all the  $N_j(t)$  particles in the set

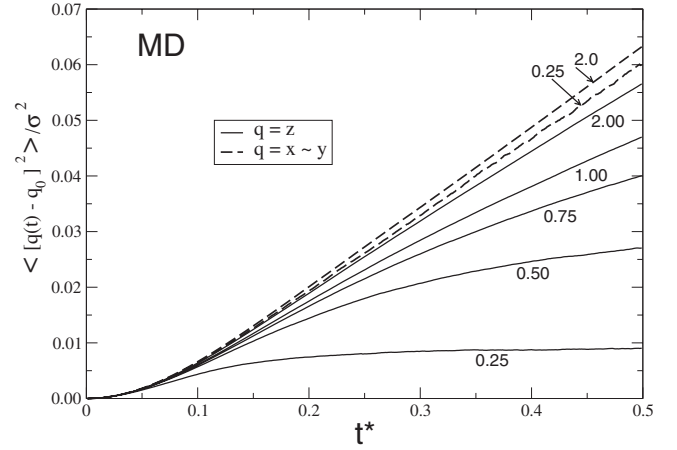


FIG. 2. Effect of the layer width  $L$  on the MD mean-square displacement as a function of reduced time  $t^*$ , in  $z$  regions away from the walls, at  $z_a=20\sigma$ , corresponding to the bulk. Continuous lines are the perpendicular  $z$  MSD, for layers of width  $L/\sigma=2.0, 1.0, 0.75, 0.50$ , and  $0.25$  as labeled. Dashed lines are the parallel  $x$  and  $y$  MSD, for layers of width  $L/\sigma=2.0$  and  $0.25$ . Conditions are the same as Fig. 1.

$$\langle [q(t) - q(0)]^2 \rangle_j = \frac{1}{N_j(t)} \sum_i^{N_j(t)} [q_i(t) - q_i(0)]^2. \quad (10)$$

The average MSD is

$$\langle [q(t) - q(0)]^2 \rangle = \frac{1}{J} \sum_j \langle [q(t) - q(0)]^2 \rangle_j. \quad (11)$$

Notice that, according to the result in Eqs. (6)–(8), this expression holds not only for  $x$  and  $y$  directions but also for the perpendicular  $z$  direction.

In Fig. 2, we show the effect of the layers width  $L$  on the MSDs, as a function of the MD reduced time,  $t^* = \sqrt{\epsilon_{FF}/m\sigma^2}t$ . The labels indicate the width  $L/\sigma=2.0, 1.0, 0.75, 0.50$ , and  $0.25$ , for the  $z$  perpendicular direction (continuous lines) and  $L/\sigma=2.0$  and  $0.25$ , for the  $x$  and  $y$  parallel directions (dashed lines). The data shown correspond to layers in the bulk, in  $z$  regions away from the walls, at  $z=20\sigma$ . We can see that the parallel  $x$  and  $y$  mean-square displacements are identical and they are fairly independent of the layer width  $L$ . For low values of  $L$ , the perpendicular MSD differs appreciable from the parallel quantities. But, since we are in the bulk region, as  $L$  increases it tends to the parallel value. It should be noted that for  $L$  as high as  $2\sigma$ , the  $z$  MSD becomes rapidly linear with time. However, for narrower layers, say  $L=0.25\sigma$ , the perpendicular MSD reaches a saturation or plateau value for large times. This is the expected result since a particle in a layer cannot have a net displacement larger than the layer width; therefore, the MSDs are bounded, i.e.,  $\text{MSD} \ll L^2$ . In other words, most particles escape the layer before the MSD reaches its linear regime.

A useful quantity, when studying particles moving in a virtual absorbing narrow layer, is the so-called *survival probability*. It measures the average probability that after a time interval  $t$  a particle still remains inside the layer. In the dif-

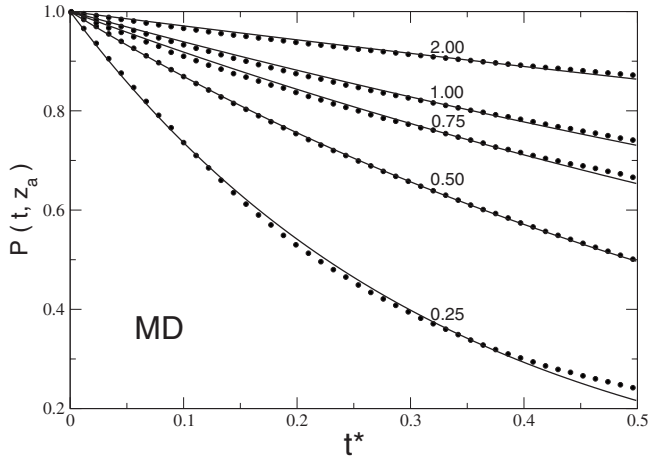


FIG. 3. Effect of the layer width  $L$  on the survival probability  $P(t, z_a)$ , as a function of the reduced time  $t^*$ , in  $z$  regions at  $z_a = 20\sigma$ , corresponding to the bulk. Labels and conditions are the same as those of Fig. 1. The dot points are the MD simulation results. The solid lines are the numerical fit with the expression  $P(t, z_a) = e^{-t/\tau(z_a)}$ .

fusion domain  $z_a \leq z < z_a + L$ , the survival probability  $P(t, z_a)$  is defined as

$$P(t, z_a) = \int_{z_a}^{z_a+L} dz \int_{z_a}^{z_a+L} dz_0 P(z, t | z_0) g(z_0). \quad (12)$$

In our MD notation,  $P(t, z_a)$  is obtained by averaging  $P_j(t) = N_j(t)/N_j(0)$  over the  $J$  repetitions

$$P(t, z_a) = \frac{1}{J} \sum_{j=1}^J P_j(t) = \frac{1}{J} \sum_{j=1}^J \frac{N_j(t)}{N_j(0)}. \quad (13)$$

In Fig. 3, we show the effect of the layer width  $L$  on survival probability  $P(t, z_a)$ , as a function of time, in  $z$  regions at  $z_a = 20\sigma$ . Labels and conditions are the same as those of Fig. 1. The dot points are the MD simulation results, according to Eq. (13). The solid lines are the numerical fit with the expression

$$P(t, z_a) = e^{-t/\tau(z_a)}, \quad (14)$$

where  $\tau(z_a)$  is a  $z_a$ -dependent relaxation time used as the only fitting constant, for each  $L$ . We shall refer to  $\tau_{MD}(z_a)$  as the MD mean exit time. The fit is good, even for layers as narrow as  $0.25\sigma$ . The rapidly decreasing survival probability for narrow layers as time increases is in agreement with the results of Fig. 2.

It should also be noted that there is an important difference among our expressions and those proposed by Liu *et al.* (LHB) [1] since the normalization factor in the denominator in LHB is  $N_j(0)$  and not  $N_j(t)$ , as in our Eq. (10). Comparing with Eq. (14) of LHB [1], we can write in our notation,

$$\langle [q(t) - q(0)]^2 \rangle_j^{LHB} = \frac{1}{N_j(0)} \sum_i^{N_j(t)} [q_i(t) - q_i(0)]^2. \quad (15)$$

Then Eq. (10) can be written as

$$\langle [q(t) - q(0)]^2 \rangle_j = \frac{1}{P_j(t)} \langle [q(s) - q(0)]^2 \rangle_j^{LHB}, \quad (16)$$

and Eq. (11) can be rewritten as

$$\langle [q(t) - q(0)]^2 \rangle = \frac{1}{J} \sum_{j=1}^J \frac{\langle [q(t) - q(0)]^2 \rangle_j^{LHB}}{P_j(t)}. \quad (17)$$

When applied for the parallel directions  $x$  and  $y$ , this expression is in agreement with the expression used by Thomas and McGaughey and others [10,11].

In order to evaluate the nonhomogeneous behavior of the diffusion process, in the next section, we derive an alternative analytical procedure to Liu *et al.*'s [1] dual simulation approach. We calculate the elements of the friction tensor as a function of the distance to the wall. In Sec. IV, we shall use the obtained analytical MSD expression from the stochastic differential equation of the system, instead of solving it numerically, to consistently determine from a MD simulation the friction coefficient as a function of the distance to the surface.

### III. ANALYTICAL LANGEVIN EQUATION APPROACH

For the system discussed in the previous section, the anisotropic Langevin-like equation can be written as

$$\frac{d\vec{r}}{dt} = \vec{v}(t),$$

$$m \frac{d\vec{v}}{dt} = -\mathbf{Y} \cdot \vec{v} + \vec{F}_{ext} + \vec{\xi}(t). \quad (18)$$

It describes the dynamics of a fluid particle of mass  $m$  located at position  $\vec{r}$  with velocity  $\vec{v}$ , in the presence of an external force  $\vec{F}_{ext}$ .  $\mathbf{Y}$  is the friction tensor of the fluid and  $\vec{\xi}(t)$  is the usual  $\delta$ -correlated-zero-mean white noise resulting from the collisions with the rest of the fluid. Without loss of generality, the Sutherland-Einstein relationship will be invoked in the form  $\mathbf{Y} = k_B \mathbf{T} \mathbf{D}^{-1}$  to write down the friction tensor  $\mathbf{Y}$  in terms of the diffusion constant matrix  $\mathbf{D}$ . Here,  $k_B$  and  $T$  are the Boltzmann constant and temperature, respectively.

The force is calculated from the potential of mean force due to the infinite walls described before and shown in Fig. 1 for a large pore with  $H=40\sigma$ , so it has only a  $z$  component, namely,  $F(z)$ . The virtual layer formalism of Liu *et al.* [1] assumes that sampling layers parallel to the interface are sufficiently thin, so that the friction coefficients in every direction are constant within them. But also, layers must be thick enough to contain an appropriate number of molecules. Thus, particles moving in the  $x$ ,  $y$  and  $z$  directions, in a layer located at a given  $z_a$ , feel an approximately constant external force, let us say  $F(z_a)$ . The friction coefficient tensor  $\mathbf{Y}$  and the diffusion matrix  $\mathbf{D}$  are then assumed to be constant within the layer. It is important to stress out that the parallel movements are also affected by the proximity of particles to the surface since they depend on the local particle density, which is not homogeneous.

We assume the following premises in order to establish the components of matrix  $\mathbf{D}$ . First, the perpendicular component  $D_{zz}$  denoted by  $D_{\perp}$  differs from the parallel components  $D_{xx}$  and  $D_{yy}$  denoted by  $D_{\parallel}$ . These parallel diagonal elements are equal, while the off-diagonal elements  $D_{xy}$  and  $D_{yx}$  are set equal to zero since the dynamics of the particles along  $x$  and  $y$  directions are undistinguishable and independent of each other. In addition, the perpendicular movement is unaffected by the parallel diffusion; thus, the nondiagonal elements  $D_{zx}$  and  $D_{zy}$  are also set equal to zero. The presence of a potential of mean force along  $z$  induces a local change in the particle density and modifies the dynamics not only in the  $z$  direction but also in the  $x$  and  $y$  directions; therefore, both  $D_{\perp}$  and  $D_{\parallel}$  are functions of  $z$ . We believe that this effect could also give rise to small but nonzero nondiagonal  $D_{xz} = D_{yz}$  elements. Such generalization merits further investigation. However, within the scope of this work and for simplicity, we shall consider a diagonal friction matrix, as in previous work [1,10,11]. If we let  $q$  and  $v_q$  be the coordinate and velocity, respectively, of a given diffusing particle, Eqs. (18) then reduce to

$$\frac{dv_q}{dt} + \alpha_q v_q = \frac{1}{m} [F(q) + \xi(t)], \quad (19)$$

where  $\alpha_q = \gamma_{qq}/m = k_B T / D_{qq} m$  with  $D_{qq}$  and  $F(q)$  being one of the diagonal elements of the diffusion matrix and the external force in the  $q$  direction, respectively. This can be solved directly as

$$v_q(t) = v_q(0)e^{-\alpha_q t} + \frac{1}{m} e^{-\alpha_q t} \int_0^t [F(q) + \xi(s)] e^{\alpha_q s} ds. \quad (20)$$

To complement the MD results of previous section, the next step is to determine the analytical MSD from the stochastic differential equation of the systems (18) in terms of the diffusion constants. The whole idea is to rewrite the Langevin equation as a differential equation for the MSD. So, let  $\Delta q = q(t) - q(0)$  and use the fact that  $\Delta q(d\Delta q/dt) = (1/2)d(\Delta q^2)/dt$  and  $\Delta q(dv_q/dt) = (1/2)[d^2(\Delta q^2)/dt^2] - v_q^2$ , to rewrite the original Langevin equation as

$$\frac{d^2 \Delta q^2}{dt^2} + \alpha_q \frac{d\Delta q^2}{dt} = \frac{2\Delta q}{m} [F(q) + \xi(t)] + 2v_q^2. \quad (21)$$

Since  $\xi(t)$  is a zero-mean delta-correlated white noise, the above equation at the average yields

$$\frac{d^2 \langle \Delta q^2 \rangle_L}{dt^2} + \alpha_q \frac{d\langle \Delta q^2 \rangle_L}{dt} = \frac{2}{m} F(q) \langle \Delta q \rangle_L + 2\langle v_q^2 \rangle_L, \quad (22)$$

where the subscript  $L$  reminds that the averages should be taken on a layer of width  $L$  in the  $z$  direction, where the force is assumed, for simplicity, to be a constant.  $L$  should be chosen such that it is large enough for avoiding an excessive escape of molecules from the layer but small enough for  $F(q)$  and  $\alpha_q$  to be approximately invariant. It is also assumed that the noise averages out to zero in the layer, i.e.,  $\langle \xi \rangle_s = 0$ . In order to get analytical results, we will assume that inside the layer the force is constant along the perpendicular direction. If the external force vanishes for the parallel  $x$  and  $y$

components and  $D_{\parallel} = 0$ , the positions and velocity of the particles are unbounded. Thus, Eq. (22) reduces to the well-known free diffusion result.

The initial value problem posed in Eq. (22), i.e.,

$$\langle \Delta q^2(0) \rangle_L = \left. \frac{d\langle \Delta q^2(t) \rangle_L}{dt} \right|_{t=0} = 0, \quad (23)$$

requires the knowledge of the averages  $\langle \Delta q \rangle_L$  and  $\langle v_q^2(t) \rangle_L$ . They can be straightforwardly found from the Langevin equation through the following approximations. First, the movements in the perpendicular and parallel directions are assumed to be independent. Thus, if  $z$  denotes the perpendicular coordinate let us define  $P(z, v, t; z_0, v_0) = P(z, t; z_0)P(v, t; v_0)$  as the joint probability of finding a particle in the layer with position  $z$  and velocity  $v$  at  $t$  given that their values were  $z_0$  and  $v_0$  at  $t_0$ , respectively. Since the velocities of the particles are unbounded, we find that for  $z$  spanning the interval  $z_a \leq z < z_b$ , the average  $\langle v_q^2(t) \rangle_L$  is given by

$$\begin{aligned} \langle v_q^2(t) \rangle_L &= \int_{z_a}^{z_b} dz \int_{z_a}^{z_b} dz_0 \int_{-\infty}^{\infty} dv_q \int_{-\infty}^{\infty} dv_0 v_q^2(t) P(z, v_q, t; v_0, z_0), \\ &= P(t, z_a) \overline{v_q^2(t)}, \end{aligned} \quad (24)$$

where

$$\overline{v_q^2(t)} = \int_{-\infty}^{\infty} dv_0 \int_{-\infty}^{\infty} dv_q v_q^2 P(v_q, t; v_0), \quad (25)$$

and  $P(t, z_a)$  is the so-called survival probability inside the layer, defined before in Eq. (12). Here we assumed that the velocity probability distribution is independent of positions. In Eq. (24),  $\overline{v_q^2(t)}$  is the mean-square velocity of a particle diffusing in a fluid without spatial constraints and subjected to an external force  $F(z)$ . Similarly, the average velocity can be written as

$$\langle v_q \rangle_L = P(t, z_a) \overline{v_q(t)}. \quad (26)$$

By integration, we get the average displacement inside the layer

$$\langle \Delta q(t) \rangle_L = \int_0^t ds P(s, z_a) \overline{v_q(s)}. \quad (27)$$

The average  $\overline{v_q(t)}$  is obtained analytically integrating Eq. (20),

$$\overline{v_q(t)} = v_0 e^{-\alpha_q t} + v_F^q (1 - e^{-\alpha_q t}). \quad (28)$$

Here, we let  $v_0 = v_q(0) = \sqrt{2k_B T / m\pi}$  and defined a drift velocity  $v_F^q = F(q) / m\alpha_q$  in our problem  $v_F^x = v_F^y = 0$ .

Now, in order to get explicit expressions for  $\langle v_q^2(t) \rangle_L$  and  $\langle \Delta q(t) \rangle_L$ , we ought to know the time dependence of  $P(t, z_a)$  and  $v_q(t)$ . Figure 3 shows the dependence of the MD simulation survival probability, in a layer located at  $z = z_a$ , as a function of time. A good fit is obtained with the exponential expression  $\exp(-t/\tau_{MD})$ , even for a layer width as narrow as  $L = 0.25\sigma$ . This is in agreement with previous observations [1,10], which indicate that the survival probability for par-

ticles to remain in the layer can be approximated, with a high degree of accuracy, by an exponential decay, with a decay constant given by the inverse of a relaxation time  $\tau$  [Eq. (14)]. We then substitute this expression into those for the dispersion of  $v_q(t)$  in the layer [Eq. (24)] and for the particle layer average displacement  $\Delta q(t)$  given by Eq. (27).

Substituting Eq. (28) into Eq. (27) gives  $\langle \Delta q(t) \rangle_L$  in terms of the parameter  $\tau = \tau(z_a)$

$$\langle \Delta q(t) \rangle_L = v_F \tau (1 - e^{-t/\tau}) + (v_0 - v_F) \tau \frac{(1 - e^{-(1+\alpha_q \tau)t/\tau})}{1 + \alpha_q \tau}. \quad (29)$$

Now, we square Eq. (20), take the particle average using  $\langle \xi(s) \xi(t) \rangle = \kappa^2 \delta(t-s)$ , and substitute it back into Eq. (24) to finally get

$$\langle v_q^2(t) \rangle_L = \overline{v_q^2(t)} e^{-t/\tau}, \quad (30)$$

with

$$\overline{v_q^2(t)} = \frac{k_B T}{m} + 2v_F(v_0 - v_F) e^{-\alpha_q t} (1 - e^{-\alpha_q t}). \quad (31)$$

To get this result, the strength of the noise  $\kappa^2$  was taken as

$$\kappa^2 = 2\alpha_q [k_B T/m - v_F^2], \quad (32)$$

by requiring  $\overline{v_q^2(t)}$  to be equal to  $k_B T/m$  for large  $t$ , in order to satisfy the fluctuation dissipation theorem. Since in the parallel directions  $F(x) = F(y) = 0$ , there is no restriction on the time expended by the particles to move in those coordinates. Therefore,  $\tau_x = \tau_y \rightarrow \infty$ ,  $\langle \Delta x(t) \rangle_L = \langle \Delta y(t) \rangle_L = 0$ , and  $\langle v_x^2(t) \rangle_L = \langle v_y^2(t) \rangle_L = k_B T/m$ .

The final step is to solve Eq. (22) with the use of Eqs. (29)–(31). After a lengthy but straightforward algebra, it can be found that the MSD in the direction  $q$  is given as [21–24]

$$\langle [\Delta q(t)]^2 \rangle = f_q(t), \quad (33)$$

where, for the parallel directions  $q = x, y$ ,

$$f_q(t) = 2D_{qq} t \omega(\alpha_q, t), \quad (34)$$

and

$$\omega(\alpha_q, t) = 1 + \frac{1}{\alpha_q t} (e^{-\alpha_q t} - 1). \quad (35)$$

This expression is identical to that found for a Brownian particle in the bulk, except that here  $\alpha_x = \alpha_y$  are functions of the position  $z$ , namely,  $\alpha_q = \alpha_q(z) = k_B T / [m D_{qq}(z)]$ .

In the presence of an external force  $F(z)$ , assumed to be constant within the layer, the perpendicular  $z$  component  $f_z(t)$  has two additional terms

$$f_z(t) = f_z^B(t) + \frac{m v_F^2}{k_B T} R(t) + \frac{m v_F (v_0 - v_F)}{k_B T} S(t), \quad (36)$$

where

$$f_z^B(t) = 2D_{zz} t \frac{a}{1-a} (\omega[1] - \omega[a]), \quad (37)$$

$$R(t) = 2D_{zz} t \frac{a}{1-a} (\omega[a] - a\omega[1]), \quad (38)$$

$$S(t) = 2D_{zz} t \frac{a}{1+a} \{ (1-a)\omega[a] + (2+a)\omega[1+a] - 2\omega[1+2a] \}. \quad (39)$$

Here, we have used the notation  $a = \alpha_z \tau$ , and

$$\omega[\lambda] = \omega(\lambda, t/\tau) = 1 + \frac{\tau}{\lambda t} (e^{-\lambda t/\tau} - 1), \quad (40)$$

with  $\lambda$  having the values 1,  $a$ ,  $(1+a)$ , or  $(1+2a)$ . The function  $\omega(\lambda)$  is well behaved and characteristic of the Langevin process. It goes asymptotically to 1 for large times, and as  $\lambda t/2$  for small times. Expanding Eqs. (34) and (36) for short times, one gets the well-known ballistic term for  $x$ ,  $y$ , and  $z$  to order  $O(t^2)$ ,

$$\lim_{t \rightarrow 0} f_q(t) = D_{qq} \alpha_q t^2 = \frac{k_B T}{m} t^2. \quad (41)$$

The long-time limit for  $x$  and  $y$  is the standard free diffusion limit

$$\lim_{t \rightarrow \infty} f_q(t) = 2D_{qq} t. \quad (42)$$

It should be noticed that for large virtual layers width  $L$ , the mean exit time  $\tau$  also becomes large. Therefore, in the bulk or in the absence of an external force, namely, when  $v_F = 0$ ,  $f_z(t)$  reduces  $f_z^B(t)$ , which gives the standard result of a homogeneous system of Brownian particles, namely,  $f_z^B(t) = f_x^B(t) = f_y^B(t)$ , given by Eq. (34). This can be obtained from Eq. (37) as  $\tau \rightarrow \infty$ . However, for finite  $L$  and  $\tau$ ,  $f_z^B(t)$  is the Brownian contribution for the diffusion constrained to the sampling layer. In that case, even in the absence of an external force, the sampled particle displacements are bounded, and the large time limit of the MSD in the  $z$  direction reaches a plateau

$$\lim_{t \rightarrow \infty} f_z^B(t) = 2D_{zz} \tau. \quad (43)$$

The last two terms in Eq. (36) account for the effect of the external force  $F(z)$  on the MSD and could give a nonsaturating curve for large times.

Equation (42) is the relationship commonly used to obtain the diffusion constant in homogeneous fluids. It is also used in the LHB approach to obtain the nonhomogeneous diffusion constants in the parallel directions. However, as we shall discuss later, the complete Eqs. (34) and (36) match very well the MSD obtained from MD for the entire time interval of the layer sampling. In principle, given the MD value of  $F(z)$ , they can be used to fit numerically MD-MSD data in order to find the diffusion constant at the layer under consideration.

#### IV. ANISOTROPIC DIFFUSION CONSTANT

In this section, we put together the fundamental results of Sec. II, for the molecular-dynamics simulation in a virtual

layer, with the corresponding analytical solution of the Langevin equation obtained in the previous section. This provides a method to evaluate the anisotropic diffusion constant. As described in Sec. II, we studied a dense Lennard-Jones fluid ( $\rho^*=0.69$ ) at low reduced temperature ( $T^*=k_B T/\epsilon_{FF}=0.75$ ) next to a highly interacting 9-3 LJ smeared wall ( $k_B T/\epsilon_{FF}=1.0$ ) [14,17]. As pointed out in the work of Thomas and McGaughey [10], the width  $L$  of the layers has to be carefully chosen. It has to be small enough to have a reasonably constant force value within it but large enough to keep a sufficient number of molecules in the layer in order to preserve the statistical nature of the MD measurements. As illustrated in Fig. 2, a reasonable compromise is found at  $L=0.5\sigma$ . For large pore width  $H$  and distances away from the wall, the force vanishes, so we reach the bulk. The predicted  $D^0$  for the bulk fluid, for  $z=20\sigma$  obtained from Fig. 2, agrees with the reported value for this fluid of  $4\times 10^{-9}$  m<sup>2</sup>/s. For a layer closer to the walls, the  $x$  and  $y$  MSDs are still identical, but that for  $z$  differs substantially, due to the strongly force  $F(z)$  acting on the particles in that direction.

As can be seen in Fig. 1, the local-density profile  $\rho(z)$ , and, therefore, the mean external force  $F(z)$  present strong oscillations next to the wall. As discussed above, we have chosen these rather demanding conditions since they correspond to those previously used in a *numerical dual simulation* evaluation of the diffusion constant [10]. The main drawback is that the local external force within each sampling virtual layer is far from being a constant. This is true even for the smaller layer width  $L=0.5\sigma$  used in this work. In fact, the smooth curve for the force shown in Fig. 8 of Ref. [10] ignores the force fine structure; it is represented in our Fig. 1 simply joining the sampling points at the left boundary of each layer denoted by  $\square$  in the figure. To overcome this difficulty, we propose the use of a coarse-grained average force in each layer or simply a spatial average in the layer, i.e.,

$$\bar{F}(z_a) \approx \frac{1}{L} \int_{z_a}^{z_a+L} F^{MD}(\zeta) d\zeta, \quad (44)$$

where  $F^{MD}(\zeta)=k_B T d \ln \rho^{MD}(\zeta)/d\zeta$ . To take into account the actual fine structure of the interfacial fluid, in an approximated way, we propose the use of different windows in  $z$  space, by shifting the position of the layers. As an example, this is illustrated in the same figure by the open circle points  $\circ$ , for a layer beginning at  $z_a=1.325\sigma$ . Repeating the MD simulations for just a few shifts is enough to reproduce approximately the force profile.

Nevertheless, for layers too close to the walls, the value of  $L$  needs to be decreased, in order to keep the constant  $F(z)$  requirement reasonably valid. To avoid the exit of all particles initially in the layer, we tested the increase in the number of particles in the system from  $N=1296$  to  $N=2916$ . Even though it modifies the MSD behavior for the long-time region, it increases too much the computational times. So we chose a compromise by using  $L=0.5\sigma$  and  $N=1296$ .

The evaluation of a phenomenological quantity, such as the self-diffusion constant  $D_{qq}$ , must be carried out by fitting the MSD simulation MD data with the analytical expression

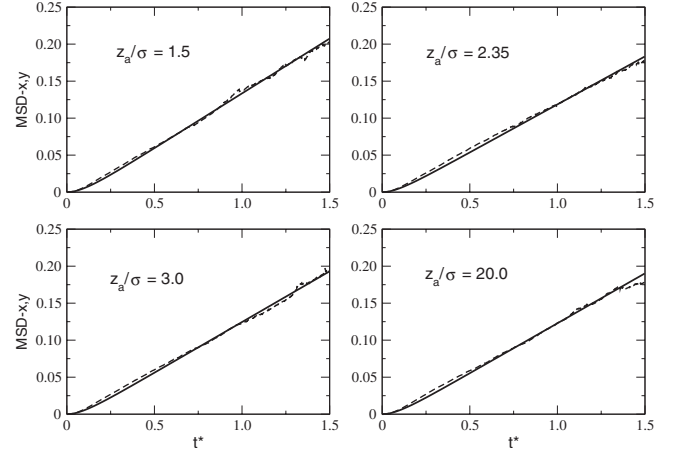


FIG. 4. Curve fit of MD parallel mean-square displacement with fitting MSD analytical expression  $f_x(t)$  given by Eq. (34), as a function of time. Curves are for  $z_a/\sigma=1.5, 2.35, 3.0,$  and  $20.0,$  as labeled.

obtained from the solution of the phenomenological Langevin equation [Eqs. (34) and (36)]. The fit for the MD parallel MSD data  $\langle[\Delta x(t)]^2\rangle$  and  $\langle[\Delta y(t)]^2\rangle$  with Eq. (34) is shown in Fig. 4, for several values of  $z$ . The fit is good and shows the expected linear  $2D_{qq}(z_a)t$  limit for large times.

An additional difficulty appears for the perpendicular diffusion. It was proven numerically by Burschka and Titulaer [25] and Harris [26] and theoretically by Razi *et al.* [27] that the conditional probability obtained as the stationary solution of the Fokker-Planck equation, associated to the Langevin equation for a system with absorbing boundaries conditions, fails to vanish at those boundaries. This inconsistency is handled in the literature shifting the boundaries away. In fact, Liu *et al.* [1] overcame this difficulty by running the dual numerical LD and MD, at different values of  $L$ , until the survival probabilities from both simulations matched. For the same  $L$ , the Langevin survival probability, as given by Eq. (14), is then known to be lower than the corresponding MD survival probability evaluated from Eq. (13). This means that for a fixed layer width, MD particles reach the boundary faster than those of LD. In other words, the Langevin dynamics mean exit time  $\tau_{LD}$ , for a given sampling layer width, is lower than the corresponding molecular-dynamics mean exit time  $\tau_{MD}$ . This is a systematic error found even for virtual absorbing layers located at the bulk. Additionally, we found that the  $\tau_{MD}$ 's were very closely proportional to  $L$ . Since the aim of this research is to predict diffusion constants from MD MSD liquid layer measurements of a given width and there is no known relation between the mean exit time and the diffusion constant under this circumstance, we therefore appeal to the simplest ansatz of fixing the layer width and shifting the mean exit time instead.

We start by evaluating the MD survival probability  $P(t, z_a)$  for the bulk fluid from Eq. (13) and the MD free diffusion bulk constant  $D^0$ . The corresponding bulk Langevin mean exit time  $\tau_{LD}^0$  is then evaluated using Eq. (36) or Eq. (43). We then conjecture that the time shift found for the bulk fluid  $\Delta\tau=\tau_{MD}^0-\tau_{LD}^0$  is approximately the same for the anisotropic fluid next to the wall, namely,

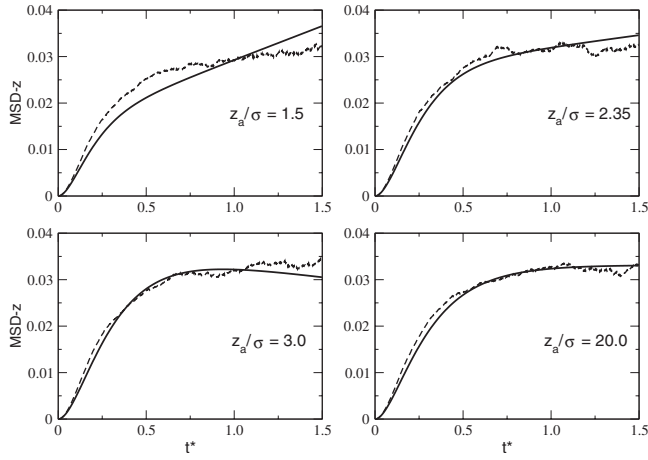


FIG. 5. Curve fit of MD perpendicular mean-square displacement with fitting MSD analytical expression  $f_z(t)$  given by Eq. (36), as a function of time. Curves are for  $z_a/\sigma = 1.5, 2.35, 3.0,$  and  $0.0$ , as labeled.

$$\tau = \tau_{LD}(z_a) = \tau_{MD}(z_a) - \Delta\tau. \quad (45)$$

Figure 5 shows the MD numerical data for the perpendicular MSD and the best fit with  $f_z(z_a)$ , for several values of  $z_a$  using Eq. (36) and ansatz (45). The fitting parameter  $D_{zz}(z_a)$  is shown in Fig. 6 along with the estimated values of  $\tau_{LD}(z_a)$  and  $\bar{F}(z_a)$  we used. We can see in Fig. 5 that for a virtual layer located at  $z_a = 20\sigma$ , the fit is good and shows that the MSD reaches an asymptotic value  $2D_{zz}\tau$  for large times. We can see that for large times, the MD data becomes noisy since most of the particles initially in the layer have already escaped. For nanometric distances to the attractive walls, the fit is still good but the effect of the drift velocity components

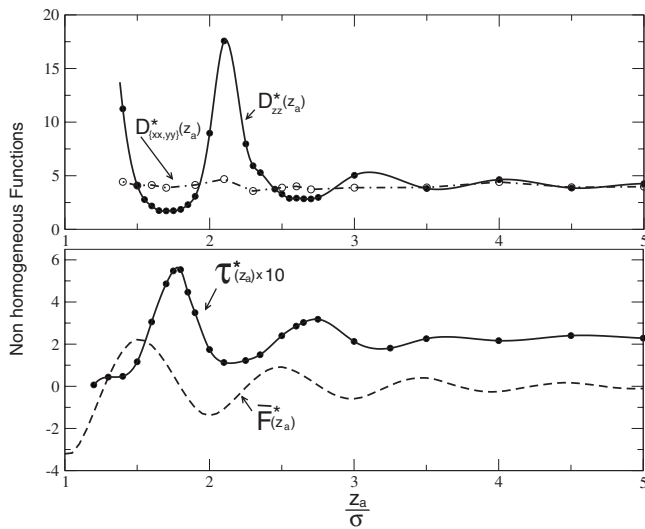


FIG. 6. Anisotropic diffusion constants  $D_{qq}(z_a)$  as a function of the sampling layer position  $z_a/\sigma$ . Also shown is the reduced Langevin dynamics mean exit time  $\tau^*(z_a)$  obtained from the MD survival probability and the approximation (45). The average reduced force  $\bar{F}^*(z_a)$  obtained from Eq. (44) is also shown.

originated by the local force becomes important. As shown in Fig. 5, a good fitting is also obtained for layers as close as  $1.5\sigma$  to the wall, but the nonconstancy of the force within the layer becomes quite apparent.

Finally, in Fig. 6, the calculated nonhomogeneous diffusion constants  $D_{qq}(z_a)$  are shown as a function of the location from the pore wall of the left boundary of the layers  $z_a/\sigma$ . Since  $D_{xx}(z_a)$  is essentially identical to  $D_{yy}(z_a)$ , we only show their mean. Close to the wall, the parallel components  $D_{xx}(z_a) = D_{yy}(z_a)$  change just a little. However, the transverse  $D_{zz}(z_a)$  shows strong oscillations. Since we are looking at a large pore of  $H = 40\sigma$ , at the center of the pore  $z_a/\sigma = 20$ , all the diffusion tensor components converge correctly to the bulk value  $D^0$ . This limit is already attained at  $z_a/\sigma = 5$  in Fig. 6. The local diffusion constant profile  $D_{zz}(z_a)$  follows inversely the shape of the local particle density  $\rho(z)$ , that is, a maximum in density gives a minimum in the perpendicular diffusion constant.

Also shown in Fig. 6 are the values of the LD reduced mean exit times  $\tau^*(z_a) = \tau_{LD}^*(z_a)$  obtained from curve fitting of the survival probability as a function of time with Eqs. (14) and (45).  $\tau_{MD}(z)$  and therefore  $\tau_{LD}(z)$  follow qualitatively very well the  $z$  dependence of the external force  $F(z)$  shown in Fig. 1. For attractive wall mean forces  $\tau(z_a) < \tau^{bulk}$  and  $P(t, z_a) < P(t)^{bulk}$ . In other words, the survival probability becomes larger or smaller than the bulk value when the local mean force gets larger or smaller than zero. Therefore, the oscillations in the local density and the local mean force modulate the diffusion of particles in regions close to the walls, as shown in Fig. 6. We also show in Fig. 6 the layer average force  $\bar{F}^*(z_a)$  used here to obtain the diffusion constants, as prescribed by Eq. (44).

## V. CONCLUSIONS

We have presented two fundamental results for the molecular-dynamics evaluation of the parallel and transverse diffusion constant in an anisotropic fluid. First, Eq. (11) or, equivalently, Eq. (17) show that the transverse  $zz$  component needs to be corrected by an extra factor, corresponding to the survival probability in the  $j$ th sampling. This is equivalent to divide by a factor  $P_j(t) = N_j(t)/N_j(0)$  not only the  $x$  and  $y$  MSD components but also the  $z$  component, as discussed in Sec. II. Equation (17) gives the connection with the prescription of LHB [1] for the parallel and perpendicular components.

Another fundamental result is the analytical solution of the anisotropic Langevin equation for the MSD [Eqs. (34) and (36)] with the correct long-time limit. Extracting the force  $F(z)$  from the MD density profiles and the mean exit time  $\tau^{MD}(z)$  from the survival probability, we can use the ansatz for  $\tau_{LD}$  [Eq. (45)] into Eq. (36) to fit the MSD numerical MD data in order to predict the transverse self-diffusion constant. So, our proposed method avoids the lengthy dual numerical Langevin molecular-dynamics simulations to match the survival probability as proposed by Liu *et al.* [1] and used by others [10,11].

Thus, we have constructed a direct and well-founded prescription for the evaluation of the anisotropic self-diffusion

constant from the molecular-dynamics mean-square displacement data. We successfully applied it to a fluid system under conditions where the local density shows marked oscillations.

#### ACKNOWLEDGMENTS

We thank our computer center (CeCalC-ULA) for the technical support and CDCHT-ULA for financing Project No. ADG-C09-95.

- 
- [1] P. Liu, E. Harder, and B. J. Berne, *J. Phys. Chem. B* **108**, 6595 (2004).
- [2] A. Morita and B. Bagchi, *J. Chem. Phys.* **110**, 8643 (1999).
- [3] R. van Zon and J. Schofield, *J. Phys. Chem. B* **109**, 21425 (2005).
- [4] S. H. Krishnan and K. G. Ayappa, *J. Chem. Phys.* **118**, 690 (2003).
- [5] C. Jun, X. F. Peng, and D. J. Lee, *J. Colloid Interface Sci.* **296**, 737 (2006).
- [6] T. Patsahan, A. Trokhymchuk, and M. Holovko, *J. Mol. Liq.* **92**, 117 (2001).
- [7] T. Demi and D. Nicholson, *Langmuir* **7**, 2342 (1991).
- [8] G. Garberoglio and R. Vallauri, *Phys. Lett. A* **316**, 407 (2003).
- [9] V. P. Sokhan, D. Nicholson, and N. Quirk, *J. Chem. Phys.* **120**, 3855 (2004).
- [10] J. A. Thomas and J. H. McGaughey, *J. Chem. Phys.* **126**, 034707 (2007).
- [11] C. D. Wick and L. X. Dang, *J. Phys. Chem. B* **109**, 15574 (2005).
- [12] P. J. Colmenares and W. Olivares-Rivas, *Phys. Rev. E* **59**, 841 (1999).
- [13] B. Sulbarán, W. Olivares-Rivas, J. C. Villegas, P. J. Colmenares, and F. López, *J. Mol. Struct.: THEOCHEM* **769**, 151 (2006).
- [14] J. Israelachvili, *Intermolecular Surface Forces*, 2nd ed. (Academic, London, 1992).
- [15] L. Smith and L. Lloyd, *J. Chem. Phys.* **71**, 4085 (1979).
- [16] D. Bratko, R. A. Curtis, H. W. Blanch, and J. M. Prausnitz, *J. Chem. Phys.* **115**, 3873 (2001).
- [17] K. P. Travis and K. E. Gubbins, *J. Chem. Phys.* **112**, 1984 (2000).
- [18] J. Reszko-Zygmunt, W. Rysko, S. Sokolowski, and Z. Sokolowska, *Colloids Surf., A* **208**, 199 (2002).
- [19] J. Santana-Solano and J. L. Arauz-Lara, *Phys. Rev. E* **65**, 021406 (2002).
- [20] W. Olivares, L. Degréve, J. C. Villegas, and M. Lozada-Cassou, *Phys. Rev. E* **65**, 061702 (2002).
- [21] C. W. Gardiner, in *Handbook of Stochastic Methods for Physics, Chemistry and the Natural Sciences*, Springer Series in Synergetics, 2nd. ed., edited by Hermann Haken (Springer-Verlag, Berlin, 1985).
- [22] D. A. McQuarrie, *Statistical Mechanics* (Harper Row, New York, 1976).
- [23] J. Keizer, *Statistical Thermodynamics of Nonequilibrium Processes* (Springer, New York, 1987).
- [24] R. K. Pathria, *Statistical Mechanics*, 2nd ed. (Butterworth Heinemann, Oxford, 1996).
- [25] M. A. Burschka and U. M. Titulaer, *J. Stat. Phys.* **25**, 569 (1981).
- [26] S. Harris, *J. Chem. Phys.* **75**, 3103 (1981).
- [27] K. R. Naqvi, K. J. Mork, and S. Waldenstrøm, *Phys. Rev. Lett.* **49**, 304 (1982).